THE ASTROPHYSICAL JOURNAL, 428:819–826, 1994 June 20

PARTICLE ACCELERATION IN AN EVOLVING ACTIVE REGION BY AN ENSEMBLE OF SHOCK WAVES

ANASTASIOS ANASTASIADIS AND LOUKAS VLAHOS
Department of Physics, University of Thessaloniki, GR-54006 Thessaloniki, Greece
Received 1993 August 6; accepted 1993 December 22

ABSTRACT

We present a model for the acceleration and transport of energetic particles (electrons and ions) inside an active region. We propose that the agent for the acceleration is an ensemble of oblique shock waves, generated inside an evolving and constantly changing active region. The acceleration is based on the "shock drift" mechanism, using the adiabatic treatment. The high-energy particles are losing energy via Coulomb collisions and radiation. We calculate the energy distribution of the particles, their acceleration time, and their maximum energy as a function of the number of shock waves present. The high-energy particles are transported inside a chaotic magnetic field and are reflected randomly when they meet a magnetic mirror point. Finally we compare our numerical results with the observations.

Subject headings: acceleration of particles — shock waves — Sun: corona — Sun: flares — Sun: magnetic fields

1. INTRODUCTION

A large fraction of the energy released during solar flares is deposited to the energetic particles (electrons or ions) and the heating of the ambient medium. High-energy particles lose their energy through radiation (X-rays, γ-rays, radio wavelengths) and cause further heating of the ambient medium.

The energy spectrum of the accelerated particles during solar flares can be found either by in situ measurements at 1 AU (e.g., Lin, Mewaldt, & van Hollebeke 1982) or by the spectral index of the emitted radiation. The observed photon spectra, for the case of ions, are fitted either to a power law or a Bessel function and for electrons are fitted to a power law, single or double, or a Maxwellian (thermal models), depending on the energy range studied (Dennis 1985, 1988; Ramaty & Murphy 1987; Vilmer 1987; Dulk, Kiplinger, & Winglee 1992). From the observations we can estimate the acceleration time and the shape of the resulting energy distribution. The process of acceleration electrons can be as small as several 100 ms or it continues up to hours. The typical value of the acceleration time for ions ranges from a few seconds up to several minutes (Ramaty & Murphy 1987). The index of the energy distribution for the ions does not vary too much from flare to flare and its characteristic value is between 3 and 4. The observed electron spectral index is highly variable and lies between 3 and 10 (Dennis 1988; Dulk et al. 1992). Interplanetary electrons escaping from the Sun and associated with solar flares have energy spectra of a double power-law type, with exponents from 0.6 to 2.0 below 100–200 keV and 2.4–4.3 above (Lin et al. 1982). It is clear that the energy distribution of electrons, accelerated in solar flares depends strongly upon the observed energy range.

In order to reproduce the energy distribution, responsible for the observed radiation, a number of acceleration mechanisms have been proposed e.g., MHD waves, shock waves, DC electric fields, double layers, or coherent acceleration processes (for reviews see Heyvaerts 1981; De Jager 1986; Forman, Ramaty, & Zweibel 1986; Vlahos et al. 1989; Ramaty & Murphy 1987; Scholer 1988; Vlahos 1989; Melrose 1990). All the above processes face a common problem: they have no clear connection to the energy release process.

The transport of energetic particles was decoupled from the acceleration processes in most studies or an artificial trap was used for the magnetic topology (Petrosian 1990; Vilmer 1993). A few attempts to integrate acceleration and transport have been made (Miller & Ramaty 1989; Ryan & Lee 1991). The processes responsible for the evolution of the particle distribution are (1) acceleration, mainly by waves (Alfvén or whistler waves), (2) energy losses due to collisions, and (3) partial trapping inside the magnetic flux tube (due to its convergence and/or the pitch angle scattering by the turbulence). Recently, following the above scenario, Hamilton & Petrosian (1992) studied the acceleration of thermal electrons, considering electron-whistler interactions in the presence of Coulomb collision losses. They argued that there must be a continuous distribution of particles present in all phases of the solar flare development and tried to give a primary acceleration mechanism for the electrons, considering different values for the characteristic energy above which the acceleration will be the dominant process. The main disadvantage in this approach is the lack of understanding for the mechanism that produces the whistler or MHD waves.

In the following section, we present a model for the evolution of the active region. We give arguments for the generation of multiple shock waves and discuss the physical processes responsible for the evolution of the injected particle distribution, inside chaotic field lines. In § 3 we give a description of our numerical model and in § 4, we present our results. Finally in § 5, we compare our results with the existing observations.

2. FORMATION AND EVOLUTION OF ACTIVE REGIONS

The acceleration of particles and their propagation is only a part of the solar flare problem. Another important part is the physics of the energy storage in an active region and its sudden release. Recently, observational evidence suggested that the energy release during flares is fragmented due to the presence of fine temporal, spatial, and spectral features of the emitted radiation (Gudel, Aschwanden, & Benz 1991; Benz & Aschwanden 1992; Vilmer 1993). In addition, during the last decade new ideas for the development of magnetic field lines above a turbulent photosphere have been proposed and more realistic magnetic topologies have been suggested (e.g., Parker 1985; van Ballegooijen 1985, 1986; Mikic, Barnes, & Schnack 1988; Priest 1992; Low 1992).

Following these ideas, some qualitative models for the energy release in solar flares, have been developed (Holman 1985; Haerendel 1987; for reviews see Vlahos 1989, 1993, 1994). Lu & Hamilton (1991) suggested that the energy released in a flare can be described in terms of "avalanche catastrophes," a process known in nonlinear, chaotic systems. Their analysis was based on the fact that the number of solar flares recorded versus the total energy, or the peak count rates using hard X-ray burst spectrometer, is given by a power law with index 1.8–1.1 (Lin & Schwartz 1987; Crosby, Aschwanden, & Dennis 1993). Following the above idea, a quantitative agreement with the energy, peak luminosity, and duration distributions, from the largest flares down to the completeness limit of the observations, was found by Lu et al. (1993).

We assume that new flux tubes from the convection zone constantly emerge or/and submerge, above the turbulent photosphere of the Sun. These tubes are fragmented in fibers with random radius and random twist. Most of these tubes are below the resolution of current instruments. The fibers are current channels which will interact with each other. The collision of the fibers can produce many discontinuous structures (e.g., neutral sheets, local E-fields, MHD waves, small-scale shock waves) and heat the ambient plasma locally (Parker 1988; Heyvaerts 1990; Heyvaerts & Priest 1992; Einaudi, Chiuderi, & Califano 1993). In Figure 1 the overall picture of complex active region is shown, where the different scales of the active regions on the Sun are presented. The production of a cascade of scales in an active region is due to the turbulent photospheric motions. The energy, in such a model, is released by means of many localized, small-scale explosive phenomena. Several authors have proposed similar concepts (e.g., Holman 1985; Haerendel 1987, 1994), and we are going to apply them here.

In most cases, the formation of neutral sheets or other types of discontinuities is randomly placed inside an active region, and the energy released may explain (partly) coronal heating. Such neutral sheets may reinforce the absorption of waves and therefore increase their efficiency in heating the corona (see Longcope & Sudan 1992).

In this paper, we assume that the active region is driven externally by a time-varying emerging flux (see, for example, Fig. 3 of Wentzel & Seiden 1992), or large-scale shear which forces many independent neutral sheets to release energy coherently. The release of energy in one neutral sheet can "remotely" trigger the nearest neighbor and so on. The energy released by a single neutral sheet is not important, nor is the independently appearing discontinuities; what is important here is that one or two neutral sheets serve as a catalyst for an organized structure to explode.

In Figure 2*a*, we sketch the active region formed by several magnetic dipoles. The emergence of new dipoles forces a number of incoherently formed neutral sheets to release energy simultaneously. Let us assume that the energy released in one neutral sheet forces others to release energy almost simultaneously, when they appear in distance shorter than a characteristic length λ_0. The "coherency length" can be estimated from the relation $\lambda_0 \simeq V_A t_0$, where t_0 is the time needed for remote triggering between two neutral sheets ($\lesssim 10\ \mathrm{s}^{-2}$) and V_A is the Alfvén velocity. Using standard parameters for the corona (see below), we estimate the Alfvén velocity to be $V_A \simeq 2 \times 10^8\ \mathrm{cm\ s^{-1}}$) and thus $\lambda_0 \simeq 10^6$ cm. Assuming that the active region has a characteristic length $\approx 10^9$ cm and the coherently interacting neutral sheets are 10^2–10^3 occupying a volume of $\simeq 10^{21}\ \mathrm{cm}^3$, then the energy release volume is a small portion of the active region. The energy released in each neutral sheet should be $\lesssim 10^{24}$ ergs for an average flare (10^{27}–10^{28} ergs). For large flares, much more complex formations are activated (e.g., interaction of larger structures). We can relate these concepts with the old ideas of "energy storage" and "trigger."

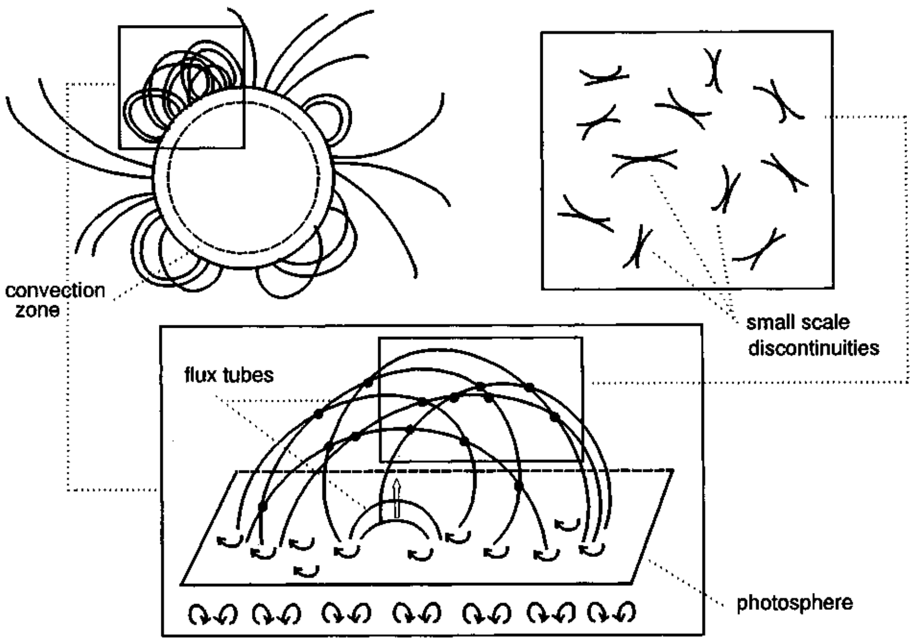

FIG. 1.—Formation of active regions and their evolution. Turbulent photospheric motions are creating a cascade of scales and producing a number of discontinuous structures in an active region.

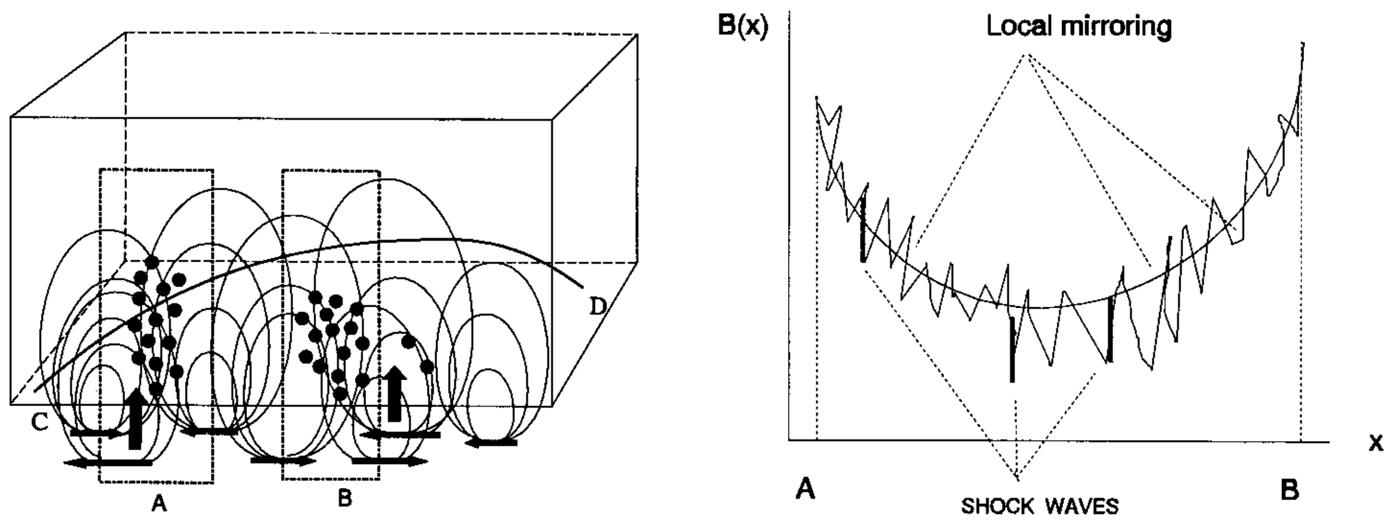

FIG. 2a FIG. 2b

FIG. 2.—The magnetic field structure inside an active region. (*a*) Due to the emergence of magnetic dipoles a number of neutral sheets are interacting coherently (areas A and B), releasing energy almost simultaneously. (*b*) The local variations of the magnetic field strength along a hypothetical line (CD), are responsible for the local mirroring of the particle.

We can summarize the key points from the above qualitative discussion as follows:

1. The emerging flux or the large-scale shear serves as an external driver which (*a*) loads the active region with magnetic flux tubes and (*b*) forces the independent neutral sheets in close proximity.
2. The remote triggering from the explosion of one neutral sheet and the forced reconnection on the neighbors is the second important point. A single explosion starts a chain of near-simultaneous explosions. The coherent appearance of many interacting neutral sheets will create a sizable explosion called microflare or flare, since it acts as a "phase transition" for a complex active region.

We assume that shock waves can be created by the intense local heating, when the plasma parameter β exceeds unity ($\beta \gg 1$) (Cargill, Goodrich, & Vlahos 1988), or when the slow shocks propagate away from the reconnecting field inside an inhomogeneous field (Ryutova, Kaisig, & Tajima 1991), or by the nonlinear evolution and breaking of reconnecting magnetic fields (Biskamp & Welter 1990). In the present study we have not included the direct acceleration of particles by the neutral sheets.

We present a model for the acceleration of energetic particles by an ensemble of oblique shock waves, which we assume to be present inside an active region when an ensemble of neutral sheets release energy coherently. The concept of particle acceleration by a number of shock waves has been applied in several astrophysical environments (e.g., Sarris 1975; Blandford & Ostriker 1980; Spruit 1988; Achterberg 1990; Gopal-Krishna & Wiita 1990; Anastasiadis & Vlahos 1993). We developed a model for the acceleration of particles (electrons and ions) by multiple shock waves for solar flare conditions without considering collisions and transport in chaotic magnetic fields (Anastasiadis & Vlahos 1991).

The basic idea in the present study is to propose a primary acceleration mechanism for the energetic particles, considering the close relation between the acceleration process, the evolving turbulent photosphere and the way the energy is released during the development of solar flares. We follow the acceleration of particles, their energy losses due to Coulomb collisions, and we include their propagation inside stochastic fields. A chaotic magnetic topology will create two types of reflection: (1) random reflection inside the active region and (2) an overall trap as the particles precipitate.

The magnetic field inside an active region formed for example by 10 or 20 randomly placed dipoles in the convection zone will create the magnetic topology shown in Figure 2. Moving along a hypothetical trajectory shown in Figure 2*a*, particles will encounter local "reflection" points and large-scale reflection (Fig. 2*b*). The small random mirrors are due to highly inhomogeneous magnetic field and the large-scale field has the tendency to become stronger as we approach the photosphere. The random mirrors reinforce the interaction with the shocks and the large-scale trapping acts as an overall mirror.

The scope of this article is to simulate the evolution of the energy distribution, inside an active region, assuming that an ensemble of oblique shock waves is present. The number of shock waves inside the active region is a free parameter. Finally we will compare our results with existing observations.

3. NUMERICAL MODEL

We simulate an active region by a box having characteristic length $L = 10^9$ cm and mean ambient magnetic field $B_0 = 10^2$ G. The ambient density is $n_0 = 10^{10}$ cm^{-3}, the plasma parameter beta is $\beta = 5$ and the Alfvén velocity is $V_A = 2.18 \times 10^8$ cm s^{-1}.

We assume that a number of shock waves (N_S) are randomly formed in a fraction of the simulation box (between $L/3$ and $2L/3$), moving with constant velocities (V_{Sj}) in random directions. These waves are considered to be small-scale ($\Delta B/B \simeq 1.2$), short-lived discontinuities, moving in random directions. Their surfaces intersect with the direction of the ambient magnetic field with different angles (θ_{Bn}). We have not included the effects of shock-shock interactions (Cargill 1991) in our study. The simulation box coincides with volumes A or B in Figure

2*a*, and the appearance of the shocks between $L/3$ and $2L/3$ with the coherently interacting neutral sheets. We evaluate the downstream parameters from the upstream ones, using the *Rankine-Hugoniot* conditions (Tidman & Krall 1971; Decker 1989). The values of the upstream parameters are $\delta_1 = 0°$, $\beta_1 = 5$, $U_1 = V_{Sj}$, $2.5 \leq M_{a1} \leq 4$, $40° \leq \theta_{Bn1} \leq 70°$, $B_1 = B_0$, where δ_1 is the angle between the direction of the upstream flow velocity U_1 and the shock normal, V_{Sj} is the velocity of the *j*th shock wave and $M_{a1} = U_1/V_A$ is the upstream Alfvénic Mach number. The M_{a1} and θ_{Bn1} are chosen randomly inside the above range. It is clear that, intermediate values of θ_{Bn} (i.e., oblique shock waves) are likely to prevail when shock waves are propagating in random field lines (Decker & Vlahos 1986).

Particles, in general, are accelerated in shock waves by either *drift* or *diffusive* mechanism (for reviews see Blandford & Eichler 1987; Jones & Ellison 1991). In the diffusive mechanism, the particle is accelerated as it scatters back and forth across the shock front by the magnetic irregularities, existing in the flow upstream and downstream (Toptyghin 1980; Jokipii 1982; Drury 1983). This mechanism is also called Fermi acceleration because of the similar nature of the Fermi process (Fermi 1949). In the drift mechanism, the particle gains energy as it drifts along the electric field at the shock front (Sarris & Van Allen 1974; Webb, Axford & Terasawa 1983; Armstrong, Pesses, & Decker 1985; Decker 1989). The diffusive shock acceleration is usually applied to the parallel and *quasi*-parallel shock waves and the drift mechanism is most promising for the case of perpendicular and *quasi*-perpendicular shocks. In the case of oblique shock wave with turbulence upstream and downstream, the acceleration of particles is probably a combination of the drift and the diffusive acceleration (Decker & Vlahos 1986).

In this study, particles (electrons and ions) are accelerated when there is a particle-shock interaction by the shock drift mechanism. We choose the shock drift mechanism since it is the only one for which analytical expressions for the energy changes exist. It is our belief that more complex processes (e.g., combination of diffusive and drift mechanism in the presence of waves) are also active but are very difficult to handle them numerically.

We use the "adiabatic treatment," in order to calculate the energy change at each particle-shock wave encounter (Webb et al. 1983; Decker 1989). The adiabatic treatment is based on the fact that the magnetic moment of the particle is conserved in a frame of reference where there is no electric field. A particle interacting with a shock can either be transmitted upstream/downstream or reflected upstream of the shock front, depending on its initial position in respect to the shock front. The pitch angle of the particle and the shock characteristics are the most important parameters in determining the acceleration process. Since the angle between the ambient magnetic field and the shock normal (θ_{Bn}) is a random parameter in our model, it is not important to follow the evolution of the particle's pitch angle at the end of each encounter. Thus, we can also choose randomly the pitch angle of each particle interacting with the shock waves.

In addition to the acceleration process, particles are subject to energy losses due to Coulomb collisions. The kinetic energy loss rate in eV s^{-1}, for the case of electrons is (Bai & Ramaty 1979):

$$\frac{dE_e}{dt} = \begin{cases} -1.55 \times 10^{-7} n_0 E_e^{-0.5} & \text{if } E_e \leq 160 \text{ keV} , \\ -3.8 \times 10^{-7} n_0 & \text{if } E_e > 160 \text{ keV} , \end{cases} \tag{1}$$

and for the case of ions is (Ryan 1986):

$$\frac{dE_i}{dt} = -7.7 \times 10^{-9} n_0 E_i^{-0.5} \quad \text{for } E_i \geq 10 \text{ MeV} , \tag{2}$$

where $E_{i,e}$ is the kinetic energy of the particle in eV and n_0 is the density in cm^{-3}. We must mention that particles can also lose energy during their interactions with the shock waves (Webb et al. 1983). The Coulomb losses are active continuously on the trajectory of the particles. On the other hand, the acceleration can occur only at the position of the shock waves (localized process). We also assume that particles are trapped at the boundaries of the simulation box, and we introduce magnetic mirroring with ratio $R_m = 0.1$. The trapping affects the trajectories of the particles, since a few will return in the acceleration site by reflection at the boundaries and thus undergo more encounters with the shock waves. The rest will escape from the simulation box. We have also investigated the role of random position mirroring on the evolution of the energy distribution. This small-scale mirroring is active downstream and upstream the shocks. Such a process, has a similar effect with the trapping of the particles in the neighborhood of shock fronts, which was studied recently by Decker (1993).

The particle population which interacts with the N_S shock waves has initially a Maxwellian distribution in the velocity space, e.g.,

$$f_j(v_j) = \frac{n_0}{(2\pi)^{1/2} V_{Tj}} \exp\left(-\frac{v_j^2}{2V_{Tj}^2}\right) , \quad j = i, e , \tag{3}$$

where v_j and V_{Tj} are the particle velocity and the thermal velocity, respectively. The kinetic energy range, we are interested in, is 2 MeV $\leq E_i \leq$ 13 MeV for the ions and 21 keV $\leq E_e \leq$ 200 keV for the electrons. The above energy ranges correspond to particles with $2 \leq (v_j/V_{Tj}) \leq 5$ for $V_{Te} = 4.19 \times 10^9$ cm s^{-1} and $V_{Ti} = 9.79 \times 10^8$ cm s^{-1}. We normalized the initial distribution in such a way that $f_j(5V_{Tj}) = 1$.

The scope of this study is to calculate the resulting energy distribution of the particles, using the numerical technique described above. In the following section we present our results in respect to the number of shock waves (N_S), which will be randomly formed inside the acceleration volume.

4. RESULTS

We consider two different models, denoted A and B. In model A the particles are trapped only by magnetic mirroring at the boundaries of the simulation box. On the other hand, in model B, particles are subject to additional trapping by a random position mirroring inside the acceleration volume.

In Figure 3, we present the time evolution of the velocity ($|v_e|/V_{Te}$) of a single electron, when there are $N_S = 80$ shock waves present, for the case of model A. In Figure 4, the time evolution of the velocity of the same electron but for $N_S = 120$ shock waves active in the acceleration volume, is shown. The variations shown in these figures, are due to the acceleration or deceleration of the electron and the Coulomb losses. When the number of shock waves is higher ($N_S = 120$), the electron stays longer ($\approx$0.2 s) inside the acceleration volume but reaches a higher energy.

The resulting energy distribution of the particles (electrons and ions) can be fitted well, with correlation coefficient $R \geq 0.8$, by a power law, e.g.,

$$F_j\left(\frac{E_j}{E_{Tj}}\right) \approx K\left(\frac{E_j}{E_{Tj}}\right)^{-s} , \quad j = i, e , \tag{4}$$

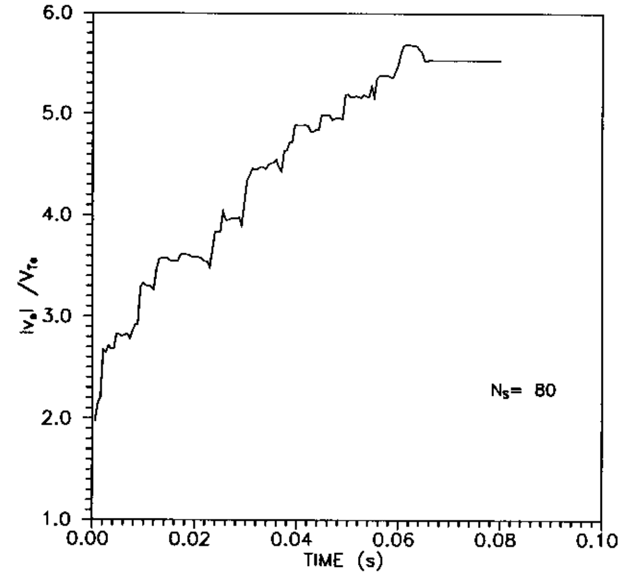

FIG. 3

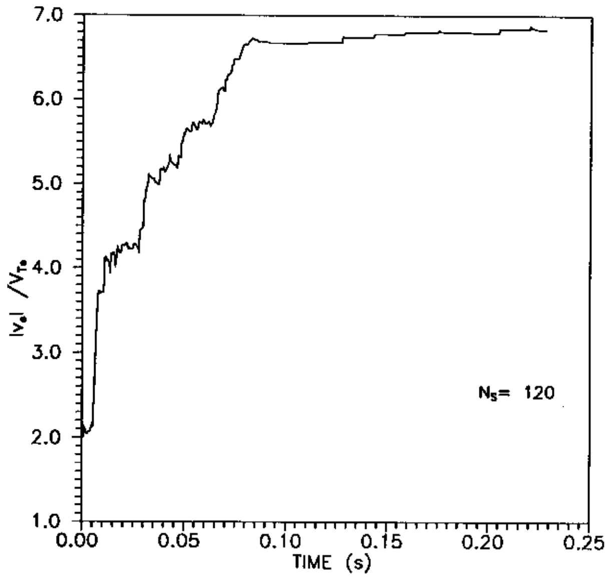

FIG. 4

FIG. 3.—The time evolution of the velocity ($|v_e|/V_{Te}$) of an electron for model A and $N_S = 80$ shock waves present in an active region
FIG. 4.—The same as Fig. 3, but for $N_S = 120$ shock waves in active region

where E_j is the kinetic energy of the particles, E_{Tj} is the thermal kinetic energy ($E_{Te} = 5$ keV for the electrons, $E_{Ti} = 500$ keV for the ions), K is a constant, and s is the power-law index. In Figure 5 we present the energy distribution for the case of electrons interacting with $N_S = 120$ shock waves for model B, having power-law index $s = 1.92$.

Our results, concerning the power-law index s of the energy distribution, the time the particle population spend inside the simulation box (t_a), the mean value of the kinetic energy reached by the most energetic particles (E_m), as a function of the number of shock waves N_S present in the active region, are given in Table 1 (for model A) and Table 2 (for model B). All these numerical results are based on the particles escaping from the acceleration volume and thus, correspond to a steady state situation.

For both models, the E_m increases as the number of shock waves been present in the active region increases. In the case of model B the particles reach higher energies, compared to model A, since they interact several times with the shock waves active. For model A the t_a remains almost constant, for ions

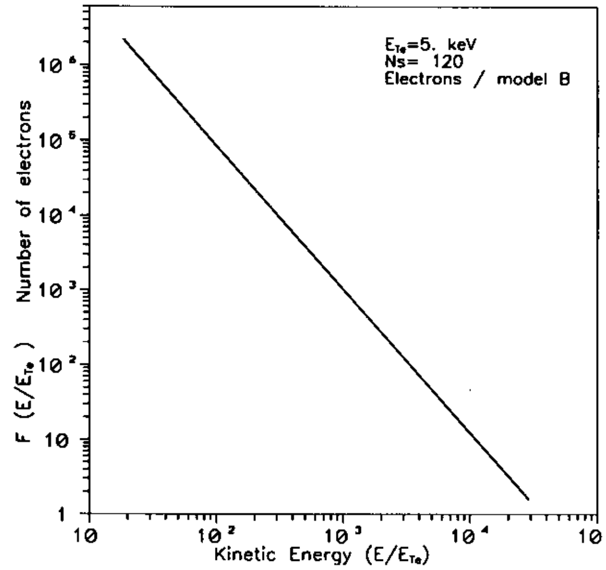

FIG. 5.—The energy distribution of power-law form, for the case of electrons for model B and $N_S = 120$ shock waves in active region.

TABLE 1

PARAMETERS FOR MODEL A

	Electrons			Ions		
N_S	s	t_a (s)	E_m (MeV)	s	t_a (s)	E_m (MeV)
10......	3.93	0.69	0.34	4.09	2.64	61
20......	3.26	0.5	1.2	3.98	2.15	137
50......	2.15	0.44	1.1	3.52	0.7	215
80......	1.71	0.38	6.6	2.8	0.61	230
100......	1.56	0.39	7.2	3.4	0.55	243
120......	2.01	0.36	9.4	3.0	0.6	250
150......	1.55	0.36	14	3.33	0.55	278
200......	1.59	0.38	8.5	3.89	0.46	304

NOTES.—Numerical results for the power-law index s, the acceleration time t_a and the mean maximum kinetic energy E_m of the particles, as a function of the number of shocks N_S, for the case of model A.

TABLE 2

PARAMETERS FOR MODEL B

	Electrons			Ions		
N_S	s	t_a (s)	E_m (MeV)	s	t_a (s)	E_m (MeV)
10......	2.51	19.4	2.7	5.61	9.89	150
20......	2.47	8.2	8	4.51	6.72	242
50......	1.58	8.8	26	4.29	2.04	305
80......	1.99	7.2	22	4.5	1.18	370
100......	1.35	6.6	37	4.19	0.97	342
120......	1.92	8.3	27	4.82	0.54	340
150......	2.05	5	22	4.68	0.56	380
200......	1.75	8.3	28	4.17	0.46	434

($t_a \approx 0.5$ s) and electrons ($t_a \approx 0.3$ s) for $N_S \geq 80$, but increases when $N_S < 80$, since the particles are not accelerated efficiently and spend more time inside the box. For model B the behavior of t_a is different. When N_S increases the acceleration time decreases for the ions. On the other hand, for electrons t_a is higher than that of model A, since they are trapped more efficiently.

The variation of the power-law index s with the number of shock waves present, for the case of ions is presented in Figure 6 and for the case of electrons in Figure 7. Notice that the variations of the power-law index for the case of ions are not significant. The mean value for model A is 3.5 and for model B is 4.5 with dispersion 0.4. On the contrary, the power-law index of the electrons for the model A is decreasing as the number of shocks is increasing up to $N_S = 80$. This is due to the fact that the environment is not an efficient accelerator and the energy distribution has softer power-law index. In the case of model B we have smaller variation of s around the mean value 1.95 with dispersion 0.37.

The time evolution of the power-law index s of the electron distribution for the case of model A, as a function of the number of shock waves, is shown in Figure 8. At early times the energy distribution has a softer index, since the particles are not accelerated to very high energies but at later times the power-law index becomes harder until it reaches its steady state value, given in Table 1.

Following Anastasiadis & Vlahos (1991), we can find that the energy density per shock is $W_S \simeq 4.12 \times 10^3$ ergs cm^{-3}. If we assume that $N_S = 200$ shock waves are present, then a large percentage of particles ($n_t \geq 10^{-2} n_0$), with velocities $\geq 2 \times V_T$, will be "energized." Under these assumptions the energy density of ions for model B is, $W_i \simeq n_t E_m \simeq 6.9 \times 10^4$ ergs cm^{-3}. It is clear that the fraction of the total energy carried by the shocks and goes to the accelerated ions is

$$P_i = \frac{W_i}{N_S \times W_S} \simeq 5.9 \times 10^{-2} . \qquad (5)$$

Using the same parameters, we can estimate that the energy given to the acceleration of electrons is

$$P_e = \frac{W_e}{N_S \times W_S} \simeq 0.5 \times 10^{-2} . \qquad (6)$$

It is obvious that less than 10% of the total energy carried by the shock waves goes to the acceleration of the particles (ions and electrons). The rest of the energy released goes to the heating of the acceleration volume.

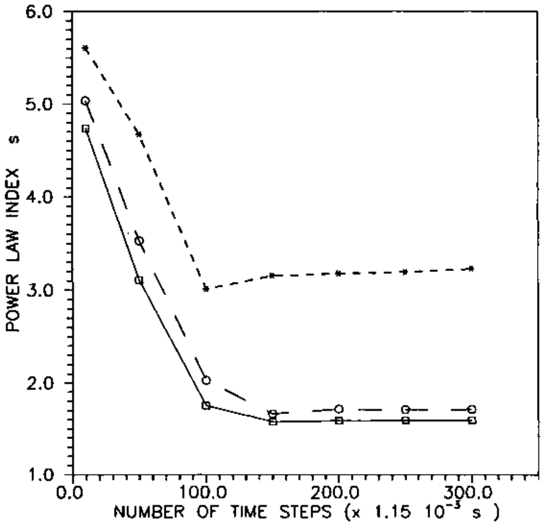

FIG. 8.—The time-dependent evolution of the power-law index s as a function of N_S for the case of electrons and model A (for $N_S = 20$ [*asterisks*], 80 [*open circles*], and 200 [*open squares*], respectively).

5. SUMMARY AND DISCUSSION

Solar flare models proposed so far were based on the assumption that a single large explosion is occurring, inside an isolated magnetic loop, or during the interaction of two arcades, or above an erupting filament. Particles were accelerated, on the basis of the above hypothesis, on a single energy

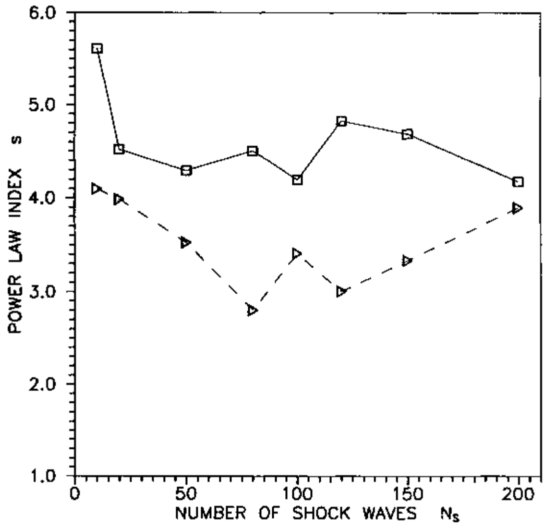

FIG. 6

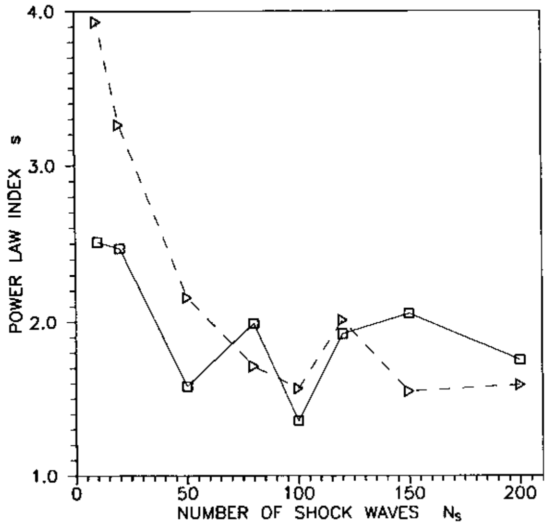

FIG. 7

FIG. 6.—The variation of the power-law index s with the number of shock waves N_S for the case of ions, for model A (△) and model B (□)
FIG. 7.—The same as Fig. 6, but for the case of electrons

release site, by assuming the existence of large-scale electric fields, large shock waves or MHD turbulence. The connection between the energy release process and the acceleration mechanism has not been studied in detail. An additional important constrain on the previous models was that the total number of particles accelerated was small compared to the required number for the interpretation of solar flares (10^{34}–10^{37} electrons above 20 keV).

In this study we followed a different approach. We considered the close relation between the evolving turbulent photosphere and the way the energy is released during the development of an active region. We assumed that the energy is released by means of many localized, small-scale explosive phenomena. A "flare" is the result of a coherent collection of such explosions, which are the drivers for the creation of a large number of discontinuities inside the active region. An ensemble of oblique shock waves (*small-scale, short-lived discontinuities*) is naturally formed in such an environment and can be the agent for the acceleration of particles. These shock waves energize a relatively large volume, so the available particles for acceleration can easily reach the numbers mentioned above.

We have not considered any shock-shock interactions in our model, through which further heating of the ambient medium of the active region can occur (Cargill 1991). We also avoided incorporating any energy losses during the propagation of the shock waves. The decay of shock waves will probably lead to the creation of MHD waves (e.g., Alfvén waves), which can accelerate particles even further. We limited our study on the evolution of a particle distribution due to the existence of N_S shock waves by considering the following processes for the particles: (1) acceleration due to the shock drift acceleration mechanism, using the adiabatic treatment, (2) energy losses due to Coulomb collisions, and (3) partially trapping by introducing magnetic mirroring, either on a large-scale (model A), or a combination of random mirroring inside the active region and global trapping (model B).

We studied numerically the dependence of the resulting energy distribution of the particles, through its power-law index s, on the number of shock waves (N_S), as well as that of the acceleration time t_a and of the mean maximum kinetic energy E_m that the particles can reach. We also followed the time evolution of the particle distribution for various number of shock waves present inside the flow of the active region.

Our main conclusions are

1. The power-law index s, of the resulting energy distribution of ions, has *a very weak dependence on the variation of the number of shock waves*, for both models A and B. The power-law index remains almost constant, with mean values, $\langle s \rangle = 3.5$ and $\langle s \rangle = 4.5$ for models A and B, respectively, where the dispersion is 0.4.

2. The power-law index s, of the resulting energy distribution of electrons for model B, shows very small variations around the mean value $\langle s \rangle = 1.95$ with dispersion 0.37, as a function of N_S. The behavior of s is different for model A, since s is decreasing as the number of waves is increasing up to $N_S = 80$, due to the fact that for $N_S \leq 80$ the acceleration is not efficient and the energy distribution has a softer index.

3. For the case of model A, the acceleration of electrons is faster ($t_a \approx 0.5$ s) than that of the ions ($t_a \approx 1$ s). In model B, as the random position mirroring affects the trajectories of the particles the acceleration times are bigger. Electrons are staying inside the acceleration box for longer time, undergoing many reflections so that t_a can be as big as 20 s, when for the ions the biggest value is ~ 10 s. Long-time acceleration needs a superposition of many similar environments where particles are constantly replenished.

4. The maximum kinetic energy E_m the particles reach is increasing with the number of shock waves active. It is clear that for model B particles are reaching higher energies as the additional magnetic mirroring affects their transport inside the acceleration volume. It is obvious that if we increase the number of shock waves present we can reach very high energies in a very small time scales.

5. The time evolution of s was studied. We found that the power-law index decreases gradually with time, since more particles interact with the shock waves and the spectrum will become harder.

6. Only a small fraction of the total energy carried by the shock waves goes to the acceleration of particles, while the rest is responsible for the heating of the acceleration volume.

We conclude that this model agrees remarkably well with the observations since (1) the index is independent of the number of shock waves for the ions. This explains the stability of the power-law index from flare to flare, (2) the low-energy electrons interact with fewer shock waves and their index is highly variable; and (3) the high-energy electrons meet a large number of shocks and their spectral index agree well with the observations close to the Sun and the in situ measurements.

It is obvious that in a complex active region a combination of accelerators may exist (e.g., localized electric field, wave activity). These processes should be studied in the future. Our contribution in this article is to present a framework on which this complexity should be used, when a better understanding of the evolution of the active region is achieved.

The present research is a part of the Ph.D. thesis of one of the authors, A. A., who would like to thank A. Achterberg, P. J. Cargill, M. Scholer, and E. T. Sarris for useful discussions on the shock wave mechanisms. We also like to thank G. Trottet, K. L. Klein, and N. Vilmer for discussions on the observation and transport of energetic particles. We acknowledge support from the European Astrophysics Doctoral Network (EADN), through the EEC ERASMUS program.

REFERENCES

Achterberg, A. 1990, A&A, 231, 251
Anastasiadis, A., & Vlahos, L. 1991, A&A, 245, 271
———. 1993, A&A, 275, 427
Armstrong, T. P., Pesses, M. E., & Decker, R. B. 1985, in Collisionless Shocks in the Heliosphere: Reviews of Current Research, ed. B. T. Tsurutani & R. G. Stone, Geophys. Monog. Ser., 35, 271
Bai, T., & Ramaty, R. 1979, ApJ, 227, 1072
Benz, A. O., & Aschwanden, M. J. 1992, in Lecture Notes in Physics, Vol. 399, Eruptive Solar Flares, ed. Z. Svestka et al. (Berlin: Springer), 106
Biskamp, D., & Welter, H. 1990, Phys. Fluids, B2, 1787
Blandford, R. D., & Eichler, D. 1991, Phys. Rep., 154, 1
Blandford, R. D., & Ostriker, J. P. 1980, ApJ, 237, 793
Cargill, P. J. 1991, ApJ, 376, 771
Cargill, P. J., Goodrich, C. C., & Vlahos, L. 1988, A&A, 189, 254
Crosby, N. B., Aschwanden, M. J., & Dennis, B. R. 1993, Sol. Phys., 143, 275
Decker, R. B. 1989, Space Sci. Rev., 48, 195
———. 1993, J. Geophys. Res., 98, 33
Decker, R. B., & Vlahos, L. 1986, ApJ, 306, 710

De Jager, C. 1986, Space Sci. Rev., 44, 43
Dennis, B. R. 1985, Sol. Phys., 100, 465
———. 1988, Sol. Phys., 118, 49
Drury, L. O'C. 1983, Rep. Prog. Phys., 46, 973
Dulk, G. A., Kiplinger, A. L., & Winglee, R. M. 1992, ApJ, 389, 756
Einaudi, G., Chiuderi, C., & Califano, F. 1993, Adv. Space Res., 13, No. 9, 85
Fermi, E. 1949, Phys. Rev., 75, No. 8, 1169
Forman, M. A., Ramaty, R., Zweibel, E. G. 1986, in Physics of the Sun, Vol. 2, ed. P. A. Sturrock et al (Dordrecht: Reidel), 249
Gopal-Krishna, & Witta, P. J. 1990, A&A, 236, 305
Gudel, M., Aschwanden, M. J., & Benz, A. O. 1991, A&A, 251, 285
Haerendel, G. 1987, Proc. 21st ESLAB Symp. (Noordwijk: ESA), SP-275
———. 1994, ApJS, 90, 765
Hamilton, R. J., & Petrosian, V. 1992, ApJ, 398, 350
Heyvaerts, J. 1981, in Solar Flare Magnetohydrodynamics, ed. E. Priest (New York: Gordon & Breach), 429
———. 1990, in IAU Symp. 142, ed. E. R. Priest & V. Krishan (Dordrecht: Kluwer), 207
Heyvaerts, J., & Priest, E. R. 1992, ApJ, 390, 297
Holman, G. D. 1985, ApJ, 293, 584
Jokippii, J. R. 1982, ApJ, 255, 716
Jones, F. C., & Ellison, D. C. 1991, Space Sci. Rev., 58, 259
Lin, R. P., Meweldt, R. A., & van Hollebeke, M. A. I. 1982, ApJ, 253, 949
Lin, R. P., & Schwartz, R. A. 1987, ApJ, 312, 462
Longcope, D. W., & Sudan, R. N. 1992, ApJ, 384, 305
Low, B. C. 1992, ApJ, 399, 300
Lu, E. T., & Hamilton, R. J. 1991, ApJ, 380, L97
Lu, E. T., Hamilton, R. J., McTiernan, J. M., & Bromund, K. R. 1993, ApJ, 412, 841
Melrose, D. B. 1990, Australian J. Phys., 43, 703
Mikic, Z., Barnes, D. C., & Schnack, D. D. 1988, ApJ, 328, 830
Miller, J. A., & Ramaty, R. 1989, ApJ, 344, 973
Parker, E. N. 1985, ApJ, 264, 642
———. 1988, ApJ, 330, 474
Petrosian, V. 1990, in IAU Symp. 142, ed. E. R. Priest & V. Krishan (Dordrecht: Kluwer), 391
Priest, E. R. 1992, in Lecture Notes in Physics, Vol. 399, Eruptive Solar Flares, ed. Z. Svestka et al. (Berlin: Springer), 15
Ramaty, R., & Murphy, R. J. 1987, Space Sci. Rev., 45, 213
Ryan, J. M. 1986, Sol. Phys., 105, 365
Ryan, J. M., & Lee, M. A. 1991, ApJ, 368, 316
Ryutova, M., Kaisig, M., & Tajima, T. 1991, ApJ, 380, 268
Sarris, E. T. 1975, Ap&SS, 36, 467
Sarris, E. T., & Van Allen, N. A. 1974, J. Geophys. Res., 79, 4157
Scholer, M. 1988, in Activity in Cool Stars Envelopes, ed. O. Havnes et al. (Dordrecht: Reidel), 195
Spruit, H. C. 1988, A&A, 194, 319
Tidman, D. A., & Krall, N. A. 1971, Shock Waves in Collisionless Plasmas (New York: Wiley)
Toptyghin, I. N. 1980, Space Sci. Rev., 26, 157
van Ballegooijen, A. A. 1985, ApJ, 294, 421
———. 1986, ApJ, 311, 1001
Vilmer, N. 1987, Sol. Phys., 111, 207
———. 1993, Adv. Space Res., 13, No. 9, 221
Vlahos, L. 1989, Sol. Phys., 121, 431
———. 1993, Adv. Space Res., 13, No. 9, 161
———. 1994, in Statistical Description of Transport in Plasmas Astro- and Nuclear Physics, ed. J. Misguich, G. Pelletier, & P. Schuck, in press
Vlahos, L., et al. 1989, in Energetic Phenomena on the Sun, ed. M. R. Kundu, B. Woodgate, & E. J. Schmahl (Dordrecht: Kluwer), 131
Webb, G. M., Axford, W. I., & Terasawa, T. 1983, ApJ, 270, 537
Wentzel, D. G., & Seiden, P. E. 1992, ApJ, 390, 280